1991ApJ...371L...1S

THE ASTROPHYSICAL JOURNAL, 371:L1–L5, 1991 April 10
© 1991. The American Astronomical Society. All rights reserved. Printed in U.S.A.

PRELIMINARY RESULTS FROM THE *COBE* DIFFERENTIAL MICROWAVE RADIOMETERS: LARGE ANGULAR SCALE ISOTROPY OF THE COSMIC MICROWAVE BACKGROUND

G. F. SMOOT,[1] C. L. BENNETT,[2] A. KOGUT,[3] J. AYMON,[1] C. BACKUS,[4] G. DE AMICI,[1] K. GALUK,[4]
P. D. JACKSON,[4] P. KEEGSTRA,[4] L. ROKKE,[4] L. TENORIO,[1] S. TORRES,[4] S. GULKIS,[5]
M. G. HAUSER,[2] M. A. JANSSEN,[5] J. C. MATHER,[2] R. WEISS,[6] D. T. WILKINSON,[7]
E. L. WRIGHT,[8] N. W. BOGGESS,[2] E. S. CHENG,[2] T. KELSALL,[2] P. LUBIN,[9]
S. MEYER,[6] S. H. MOSELEY,[2] T. L. MURDOCK,[10] R. A. SHAFER,[2] AND
R. F. SILVERBERG[2]

Received 1990 October 26; accepted 1991 January 11

ABSTRACT

The *COBE* Differential Microwave Radiometers (DMR) instrument has produced preliminary full sky microwave maps at 31.5, 53, and 90 GHz with two independent channels at each frequency. At millimeter wavelengths, the cosmic microwave background (CMB) dominates the sky brightness with an intensity more than a thousand times the foreground Galactic emission. Emission from our Galaxy is seen unambiguously at all three frequencies. The dipole anisotropy, attributed to the motion of our solar system with respect to the CMB reference frame, shows strongly in all six sky maps and is consistent with a Doppler-shifted thermal spectrum. The best fitted dipole has amplitude 3.3 ± 0.2 mK in the direction $(\alpha, \delta) = (11^{h}.2 \pm 0^{h}.2, -7° \pm 2°)$ (J2000) or $(l, b) = (265° \pm 2°, 48° \pm 2°)$. There is no clear evidence in the maps for any other large angular scale features. We place a limit of $\Delta T/T_0 < 3 \times 10^{-5}$ ($T_0 = 2.735$ K) for the rms quadrupole amplitude; for monochromatic fluctuations $\Delta T/T_0 < 4 \times 10^{-5}$; and for Gaussian fluctuations $\Delta T/T_0 < 4 \times 10^{-5}$. All limits are given at the 95% confidence level and reflect currently estimated limits on systematic effects. These measurements place the most severe constraints to date on many potential physical processes in the early universe, such as anisotropic expansion of the universe, very long wavelength gravitational waves, cosmic strings, and large-scale primordial fluctuations.

Subject headings: cosmic background radiation — cosmology — early universe

1. INTRODUCTION

Twenty-five years after its discovery the cosmic microwave background (CMB) radiation remains our most significant probe of the large-scale structure and thermal history of the universe. In the standard big bang model of cosmology, the CMB has traveled to us directly from an early epoch when the universe was roughly a thousand times smaller than the present. The last significant interaction between the CMB and matter in the universe was Thomson scattering of the CMB at a redshift of about a thousand, over a small range ($\pm 4\%$) of redshift named the surface of last scattering. A measurement of the intensity of the CMB as a function of angle on the sky represents a map of the large-scale geometry of the observable universe and the distribution of matter and energy from that early epoch. In the standard big bang model, regions of the sky separated by more than a few degrees were not causally connected at the surface of last scattering. Any structures or features appearing on larger angular scales are intrinsic and reflect fundamental features of the universe remaining from its earliest times ($z \gg 10^8$). In this *Letter*, we present preliminary, but precise, microwave maps of the sky and thus of the early universe derived as the first results from the Differential Microwave Radiometers (DMR) experiment aboard the *Cosmic Background Explorer* (*COBE*). Previous large angular scale isotropy measurements are reviewed by Partridge (1988) and Wilkinson (1986) and are compared to the DMR results in Table 2.

The DMR instrument is designed to map the CMB intensity on large angular scales. The instrument is described by Smoot et al. (1990) and its calibration techniques by Bennett et al. (1991). The instrument consists of six differential microwave radiometers, two independent radiometers at each of three frequencies: 31.5, 53, and 90 GHz, corresponding to wavelengths of 9.5, 5.7, and 3.3 mm. These frequencies were chosen to be near the minimum of the Galactic emission spectrum and near the CMB peak. The multiple frequency measurements provide the ability to separate Galactic emission from cosmic emission based on spectral shape and to measure the spectrum of detected anisotropies.

The DMR instrument measures the difference in power received from two regions on the sky that are 60° apart. Each antenna has a field of view which is approximately a 7° FWHM Gaussian (Toral et al. 1989). *COBE* (Boggess et al. 1991) is in a 900 km altitude near-polar (99° inclination) orbit which precesses to follow the terminator. Over 6 months the

[1] Lawrence Berkeley Laboratory and Space Sciences Laboratory, MS 50-232, University of California, Berkeley, CA 94720.
[2] Laboratory for Astronomy and Solar Physics, NASA/Goddard Space Flight Center, Code 685, Greenbelt, MD 20771.
[3] National Research Council, NASA/GSFC, Code 685, Greenbelt, MD 20771.
[4] ST Systems Inc., 4400 Forbes Building, Lanham, MD 20706.
[5] Jet Propulsion Laboratory, MS 169-506, 4800 Oak Grove, Pasadena, CA 91109.
[6] Massachusetts Institute of Technology, Room 20F-001, Department of Physics, Cambridge, MA 02139.
[7] Princeton University, Department of Physics, Jadwin Hall, Box 708, Princeton, NJ 08544.
[8] University of California, Los Angeles, Department of Astronomy, Los Angeles, CA 90024-1562.
[9] University of California, Santa Barbara, Department of Physics, Goleta, CA 93106.
[10] General Research Corporation, 5 Cherry Hill Drive, Suite 220, Danvers, MA 01923.

© American Astronomical Society • Provided by the NASA Astrophysics Data System

1991ApJ...371L...1S

combination of the 0.8 rpm spacecraft spin, 103 minute orbit, and 1° per day orbital precession cause the DMR antennas to observe every portion of the sky thousands of times. Each portion of the sky is linked to every other portion of the sky through highly redundant difference measurements between all fields of view which are 60° apart.

2. DMR OBSERVATIONS AND DATA PROCESSING

Data from *COBE* are digitized and stored in an on-board tape recorder before being telemetered daily to a ground station. A preprocessor strips the DMR data from the telemetry stream, merges the raw DMR data with spacecraft attitude and orbit information, and checks the quality of the data, flagging data known or suspected to be unusable. We reject data of questionable telemetry quality, data without accompanying attitude information, or with the instrument science telemetry disabled. This accounts for less than 1% of the data. We reject spikes and transients in the data, discarding all points that lie more than 5 times the RMS scatter from the daily mean (<0.1% of the data). The Moon is the only known solar system, Galactic, or extragalactic source observed by *COBE* that would exceed this limit. The next largest signal is from Jupiter and is less than 0.3 mK. The attitude control system keeps the instrument in the shade at all times with viewing angle >60° from the Sun. For this *Letter* the small effects of Jupiter and the Sun are ignored, and all data with an antenna pointed within 25° of the Moon are rejected.

We remove a mean 4 hr baseline and apply a calibration factor to convert the data from digitized telemetry units to antenna temperature. We correct the calibrated data to solar system barycenter to remove the effects of the satellite motion (7.4 km s^{-1}) around Earth and Earth's motion (30 km s^{-1}) around the solar system barycenter. The results below contain no other corrections. The calibrated data are fitted to spherical harmonic expansions and to sky maps with 6144 pixels (2°.8 angular size) whose independent antenna temperatures are chosen to minimize the χ^2 sum,

$$\chi^2 = \sum (T_i - T_j - DT_{ij})^2/\sigma_{ij}^2 ,$$

where the sum is over all observations; T_i and T_j are the map temperatures at pixels i and j, respectively; and DT_{ij} and σ_{ij} are the measured temperature differences between pixels i and j and their associated errors, respectively. Since the antenna beam width is larger than the pixel size, there is some correlation between neighboring pixels for any real signal. Further details of the data processing algorithms may be found in Torres et al. (1989).

By a week after the 1989 November 18 launch, all six channels of the DMR instrument were collecting stable data. At this time the random errors are dominated by white noise from the receivers. The noise levels are close to those measured prior to launch; the noise has a Gaussian distribution to a high degree of accuracy, with typical current RMS noise per pixel on the order of $\Delta T/T_0 \sim 10^{-4}$ and per spherical harmonic coefficient $\Delta T/T_0 \sim 3 \times 10^{-6}$ (68% confidence limit). These preliminary DMR results are limited not by this statistical uncertainty, but by our current estimates of upper limits on potential systematic effects. The *COBE* orbit provides full sky coverage but could also introduce spurious modulation of the signal correlated with antenna pointing (e.g., from changes in local magnetic field or instrument temperature). Intermittent local foreground signals in the antenna sidelobes may introduce features (e.g., Earth emission, diffracted solar radiation, or Moon emission). The data reduction process itself, including the subtraction of the instrumental baseline, could also lead to the addition or subtraction of features in the maps.

A variety of techniques exist to identify potential systematic errors and place limits on their effects. The most general technique is a least-squares fit to the time-dependent effect in the calibrated data. As a cross-check, and for instances where the time dependence is not known *a priori*, upper limits may be derived through differencing sky maps produced when the systematic effect is known to be at different strengths. The degree to which the subtracted maps differ from instrumental noise provides a limit to the effect on the DMR sky maps.

Table 1 lists preliminary 95% confidence limit upper limits to potential systematic effects in the maps for each of the DMR channels. The largest is the absolute calibration of the instrument, currently uncertain to 5%. The uncertainty in absolute calibration does not create artifacts in the maps but affects the calculated amplitude of existing features (e.g., the dipole anisotropy). We are continuing to obtain and analyze calibration information and anticipate improved calibration in the future. The next largest effect is the modulation of the instrument output in Earth's magnetic field; the primary effect is upon the dipole term of a spherical harmonics expansion. The magnetic effects will be modeled and removed in future analysis. The A channel at 53 GHz unambiguously shows this effect; we do not include the 53A channel in the results presented below. The largest potential effects upon the quadrupole term are Earth emission and the possibility of undetected calibration drifts. The current 95% confidence limit upper limits on the combined systematic errors are $\Delta T/T_0 < 8 \times 10^{-5}$ for the dipole anisotropy and $\Delta T/T_0 < 3 \times 10^{-5}$ for the quadrupole and higher order terms. Unless stated otherwise, all uncertainties are 95% confidence level; we use a value $T_0 = 2.735$ K (Mather et al. 1990; Gush, Halpern, & Wishnow 1990). As the DMR gathers redundant sky coverage and the analysis continues, we will produce refined estimates of, or limits on, these effects. It is important to note, however, that the DMR is free from some of the systematics of previous large-scale sky surveys. Two independent full sky maps at each of three frequencies, with rapid and highly redundant sky coverage, present a powerful tool for analysis and removal of possible systematic effects.

In addition to the effects listed in Table 1, various celestial sources present in the sky (e.g., planets, the Galaxy, and extragalactic sources) will create anisotropies in the sky not of cosmological origin. These are generally small. We estimate that Galactic emission is less than 0.13 mK at Galactic latitude $|b| > 10°$ at 53 and 90 GHz.

3. RESULTS

Figure 1 (Plate L1) shows six maps of the entire sky in Galactic coordinates. The readily observable features in these maps are the dipole anisotropy and emission from the Galactic plane. Galactic emission is visible in the maps at all three frequencies at approximately the level estimated prior to flight. We have fitted the individual maps and the raw data directly for a dipole and a dipole plus quadrupole anisotropy, excluding data where $|b| < 10°$. Fitted parameters and formulation are shown in Table 2. The only large angular scale anisotropy detected to date is the dipole anisotropy. We consider some sample potential anisotropies in more detail.

Movement at a speed $\beta = v/c$ relative to an isotropic blackbody radiation field of temperature T_0 produces a Doppler-

© American Astronomical Society • Provided by the NASA Astrophysics Data System

1991ApJ...371L...1S

© American Astronomical Society • Provided by the NASA Astrophysics Data System

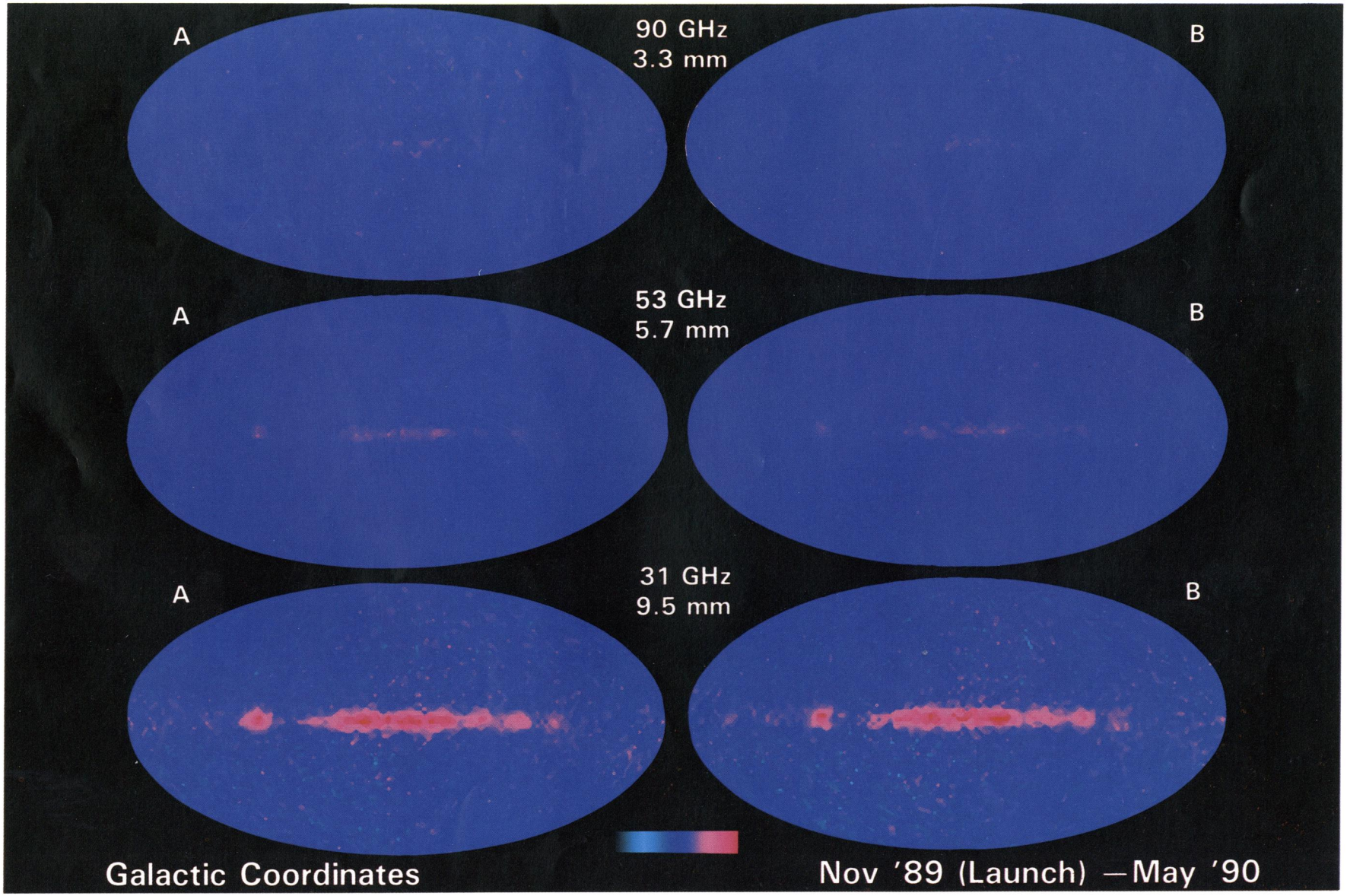

FIG. 1.—*COBE* DMR full sky maps of the relative temperature of the sky at frequencies of 31.5, 53.0 and 90.0 GHz corresponding to wavelengths of 9.5, 5.7, and 3.3 mm. The color scale corresponds to an intensity variation of about 0.15%. The maps are in Galactic coordinates with the center of the Galaxy in the center of the maps and the plane of the Galaxy horizontal. The maps are Hammer-Aitoff equal area projections. The two noticeable features of the maps are (1) the dipole anisotropy, which manifests itself as a smooth variation from warmer to cooler going from the upper right to the lower left; and (2) emission from the Galactic plane. The dipole amplitude is nearly independent of frequency while the Galactic signal is not. The maps have been translated to the solar system barycenter by correcting for the effect of the satellite and Earth orbital velocities.

SMOOT et al. (see 371, L2)

1991ApJ...371L...1S

TABLE 1

PRELIMINARY 95% CONFIDENCE LEVEL UPPER LIMITS TO SYSTEMATIC EFFECTS IN DMR MAPS (mK)

EFFECT	CHANNEL					
	31A	31B	53A	53B	90A	90B
Signals						
Earth	0.070	0.070	0.040	0.040	0.040	0.040
Moon (>25°)	0.004	0.004	0.004	0.004	0.004	0.004
COBE shield and Dewar	0.002	0.002	0.002	0.002	0.002	0.002
Sun	0.001	0.001	0.001	0.001	0.001	0.001
Environmental Susceptibilities						
Magnetic (dipole)	0.077	0.100	0.260	0.034	0.143	0.059
Magnetic (quadrupole)	0.014	0.017	0.022	0.024	0.079	0.006
Thermal	0.012	0.010	0.012	0.010	0.009	0.007
Voltage	0.010	0.010	0.010	0.010	0.010	0.010
Cross-talk	0.0001	0.0001	0.0001	0.0001	0.0001	0.0001
Software and Calibration						
Absolute calibration[a]	0.165	0.165	0.165	0.165	0.165	0.165
Calibration drift	0.043	0.079	0.031	0.033	0.049	0.039
Antenna pointing	0.030	0.030	0.030	0.030	0.030	0.030
Base drift	0.012	0.033	0.005	0.005	0.009	0.006
Solution stability	0.0001	0.0001	0.0001	0.0001	0.0001	0.0001
Total systematics, dipole	0.20	0.23	0.32	0.18	0.23	0.19
Total systematics, $l \geq 2$	0.09	0.12	0.07	0.07	0.11	0.07

[a] Dipole term only.

TABLE 2

DIPOLE AND QUADRUPOLE ANISOTROPY PARAMETERS

COEFFICIENT	AMPLITUDE (mK)			
	DMR[a]	Berkeley[b]	Princeton[c]	Relict[d]
T_0 (mK)	2735 ± 60[e]			
D_x (mK)	-3.24 ± 0.20[f]	-3.37 ± 0.17	-3.07 ± 0.17	-3.08 ± 0.10
D_y (mK)	0.67 ± 0.13[f]	0.63 ± 0.09	0.67 ± 0.09	0.57 ± 0.05
D_z (mK)	-0.40 ± 0.13[f]	-0.49 ± 0.09	-0.45 ± 0.09	-0.44 ± 0.05
Q_1 (mK)	-0.03 ± 0.07[g]	0.21 ± 0.09	0.15 ± 0.08	-0.02 ± 0.03
Q_2 (mK)	0.02 ± 0.07[g]	0.27 ± 0.10	0.15 ± 0.11	0.04 ± 0.03
Q_3 (mK)	-0.03 ± 0.07[g]	0.16 ± 0.11	0.13 ± 0.07	-0.02 ± 0.03
Q_4 (mK)	-0.05 ± 0.07[g]	-0.10 ± 0.09	-0.06 ± 0.11	0.05 ± 0.02
Q_5 (mK)	0.02 ± 0.07[g]	0.05 ± 0.08	-0.01 ± 0.07	-0.15 ± 0.04
D[h] (mK)	3.3 ± 0.2[f]	3.44 ± 0.21	3.18 ± 0.21	3.16 ± 0.12
$\alpha(h)$	11.2 ± 0.2[f]	11.2 ± 0.2	11.2 ± 0.2	11.3 ± 0.2
δ	$-7° \pm 2°$[f]	$-6° \pm 1°.5$	$-8° \pm 2°$	$-8° \pm 2°.5$
Q_{rms}[i] (mK)	<0.07[g]	<0.2	<0.2	<0.08

NOTE.—$T(\alpha, \delta) = T_0 + D_x \cos\delta\cos\alpha + D_y \cos\delta \sin\alpha + D_z \sin\delta + Q_1(3\sin^2\delta - 1)/2 + Q_2 \sin 2\delta\cos\alpha + Q_3 \sin 2\delta \sin\alpha + Q_4 \cos^2\delta \cos 2\alpha + Q_5 \cos^2\delta \sin 2\alpha$.

[a] DMR: this *Letter*.

[b] Berkeley: Lubin et al. 1985.

[c] Princeton: Fixsen, Cheng, & Wilkinson 1983.

[d] Relict: Strukov & Skulachev 1988. Our analysis for quadrupole values.

[e] Mather et al. 1990.

[f] 95% confidence limit estimated systematic error limits including calibration error.

[g] 95% confidence limit estimated systematic error limits.

[h] $D^2 = D_x^2 + D_y^2 + D_z^2 = 3D_{rms}^2$; celestial coordinates epoch J2000 for DMR.

[i] $Q_{rms}^2 = 4/15\,(3/4Q_1^2 + Q_2^2 + Q_3^2 + Q_4^2 + Q_5^2)$. Limits are 95% confidence limit.

© American Astronomical Society • Provided by the NASA Astrophysics Data System

1991ApJ...371L...1S

shifted temperature distribution (Peebles & Wilkinson 1968), which can be expanded in powers of β:

$$T(\theta) = T_0(1-\beta^2)^{1/2}/(1-\beta\cos\theta)$$
$$\sim T_0[1+\beta\cos\theta+(\beta^2/2)\cos 2\theta+O(\beta^3)] .$$

The monopole term is the temperature of the CMB without the Doppler shift. The first-order term in β is a dipole distribution, which varies as the cosine of the angle θ between the direction of observation and the velocity. The second-order term in β is a quadrupole, which varies as the cosine of twice the angle with an amplitude $\beta/2$ times the dipole amplitude. The spectrum of all the published dipole parameters, including those from the FIRAS experiment (Cheng et al. 1990), are consistent with a Doppler-shifted blackbody origin.

Accepting the interpretation that the dipole anisotropy is due to the Doppler shift of our motion relative to the CMB radiation field, the DMR–determined speed is $\beta = 0.00122 \pm 0.00006$ or $v = 365 \pm 18$ km s^{-1} (using $T_0 = 2.735$ K). The dipole results and the maps shown are in the solar system barycenter frame. Assuming that the local standard of rest moves at 220 km s^{-1} toward the direction $l = 90°$, $b = 0°$ (Fich, Blitz, & Stark 1989) and that the solar system motion with respect to the local standard of rest is 20 km s^{-1} toward $l = 57°$, $b = 23°$ (Kerr & Lynden-Bell 1986), the derived peculiar motion of the Galaxy is $v_g = 547 \pm 17$ km s^{-1} in the direction $l = 266° \pm 2°$ and $b = 29° \pm 2°$. Using a solar motion relative to the Local Group of galaxies of 308 km s^{-1}, toward $l = 107°$ and $b = -7°$ (Yahil, Tamman, & Sandage 1977), the velocity of the Local Group of galaxies is $v_{lg} = 622 \pm 20$ km s^{-1} in direction $l = 277° \pm 2°$ and $b = 30° \pm 2°$.

A general multipole expansion fitting to the data and maps is of the form

$$T(\theta,\phi,\nu) = \sum_l \sum_{m=-l,l} a_{lm}(\nu)Y_{lm}(\theta,\phi)$$
$$= \sum_l \sum_{m=-l,l} a_{lm}(\nu)\left[\frac{(2l+1)(l-|m|)!}{4\pi(l+|m|)!}\right]^{1/2} \times P_l^{|m|}(\cos\theta)e^{im\phi} ,$$

where the $Y_{lm}(\theta,\phi)$ are the orthonormal spherical harmonics and ν is frequency. However, since the temperature T must be real, we use

$$T(\theta,\phi) = \sum_l \sum_{m=0,l} [b_{lm}\cos(m\phi) + b_{l-m}\sin(m\phi)] \times k\left[\frac{(2l+1)(1-m)!}{4\pi(l+m)!}\right]^{1/2} P_l^m(\cos\theta) ,$$

where $k = \sqrt{2}$ for $m \neq 0$ and $k = 1$ for $m = 0$; $P_l^m(\cos\theta)$ are the associated Legendre functions, and thus

$$a_{lm}(\nu) = \frac{1}{\sqrt{2}}[b_{lm}(\nu) - ib_{l-m}(\nu)] ,$$

$$a_{l-m}(\nu) = \frac{(-1)^m}{\sqrt{2}}[b_{lm}(\nu) + ib_{l-m}(\nu)] ,$$

and the b_{lm} are real numbers. We have fitted both the data and the maps, excluding the region contaminated by the Galactic plane, to obtain the b_{lm} to order $l = 20$.

Figure 2 (Plate L2) shows the maps with the fitted dipole anisotropy subtracted. There is no visible evidence for any emission features other than the Galaxy, which is primarily localized to the Galactic plane. We have made a series of fits and searches with various cuts in Galactic latitude. We find a limit on

$$Q_{\rm rms} = \langle(\Delta T)^2_{\rm quadrupole}\rangle^{1/2} = \left(\frac{1}{4\pi}\sum_m |b_{2m}|^2\right)^{1/2}$$

corresponding to $Q_{\rm rms}/T_0 = (\Delta T/T_0)_{\rm rms} < 3 \times 10^{-5}$ (95% confidence limit).

The CMB fluctuation correlation function is defined as $C(\alpha) = \langle T(\boldsymbol{n}_1)T(\boldsymbol{n}_2)\rangle$, where $\boldsymbol{n}_1 \cdot \boldsymbol{n}_2 = \cos\alpha$ and $C(\alpha)$ is the average over all pairs of points in the sky separated by angle α. Using the addition theorem for spherical harmonics, we can express the limits on the higher order moments in terms of the power spectra of the coefficients or the correlation function:

$$C(\alpha) = \frac{1}{4\pi}\sum_l \left(\sum_m |a_{lm}|^2\right)P_l(\cos\alpha)$$
$$= \frac{1}{4\pi}\sum_l \left(\sum_m |b_{lm}|^2\right)P_l(\cos\alpha) ,$$

where $P_l(\cos\alpha)$ is the Legendre polynomial of order l. Excluding components of $l = 0$ (monopole), $l = 1$ (dipole) and $l > 20$, we find $|C(\alpha)| < 0.01$ mK^2 (95% confidence limit) for the range $15° < \alpha < 165°$, corresponding to

$$\left\langle \frac{\Delta T(\boldsymbol{n}_1)}{T_0}\frac{\Delta T(\boldsymbol{n}_2)}{T_0}\right\rangle < 10^{-9} .$$

Monochromatic limits are those which present a pattern covering the full sky and are computed from the spherical harmonic amplitudes in a manner similar to the correlation function,

$$(\Delta T_l)^2 = \frac{1}{4\pi}\sum_m |b_{lm}|^2 .$$

The DMR data provide a limit of $\Delta T_l/T_0 < 4 \times 10^{-5}$ (95% confidence limit) for monochromatic effects.

If there are Gaussian fluctuations in the CMB, the pixel-to-pixel variance observed is the quadrature sum of the receiver noise and the intrinsic Gaussian fluctuation on the sky:

$$\sigma_i^2 = \sigma_{i\,\rm DMR}^2 + \sigma_{\rm Sky}^2 .$$

Using the instrument noise per pixel, $\sigma_{i\,\rm DMR}^2$, estimated through differencing the independent maps for each frequency, we compute the mean intrinsic sky fluctuation, $\sigma_{\rm Sky}$, resulting in the Gaussian fluctuation limit $\Delta T/T_0 < 4 \times 10^{-5}$ (95% confidence limit).

4. DISCUSSION

The limits reported here relate directly to the large-scale geometry and dynamics of the universe. The Hubble expansion of the early universe was uniform to one part in 10,000. The large-scale geometry of the universe is well described by a Robertson-Walker metric from the surface of last scattering to the present. While the limit is very model dependent, we can conclude that the universe is rotating less than 3×10^{-24} rad s^{-1}, or less than 1/10,000 of a turn in the last 10 billion years (Barrow, Juszkiewicz, & Sonoda 1985; Collins & Hawking 1973). The DMR results place a statistical limit on the possible energy density of long-wavelength gravity waves which, expressed as a ratio of the energy density to the critical density, is $\Omega_{\rm GW} < 0.1(\lambda_{\rm GW}/1\ {\rm Mpc})^{-2}$ (Burke 1975). These results imply that any cosmic strings with angular size 20° or greater must have mass per unit length μ such that $G\mu/c^2 < 10^{-5}$ (95% confidence limit) (Stebbins 1988). The amplitude of density

© American Astronomical Society • Provided by the NASA Astrophysics Data System

1991ApJ...371L...1S

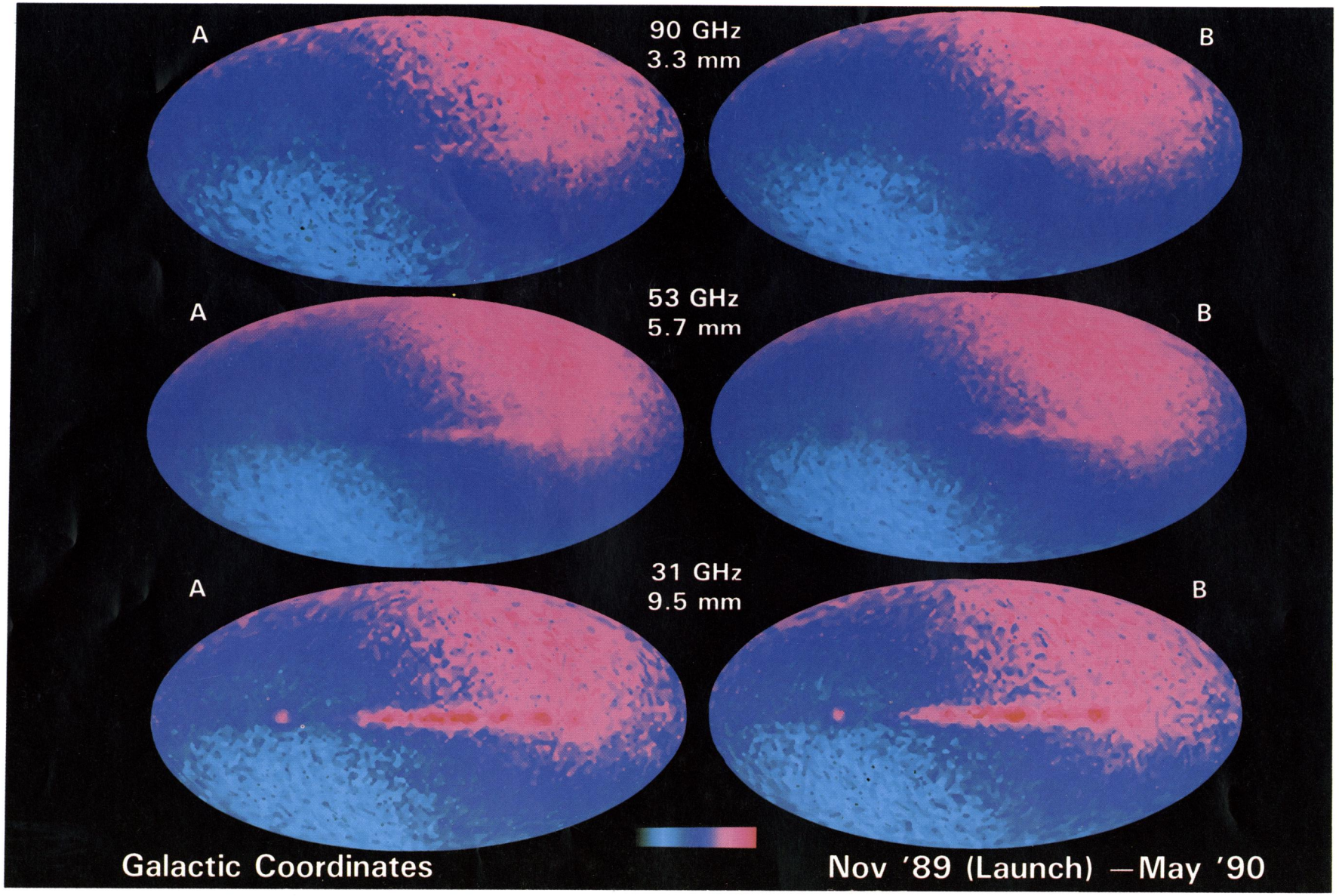

FIG. 2.—*COBE* DMR full sky maps of the relative temperature of the sky at frequencies of 31.5, 53.0 and 90.0 GHz corresponding to wavelengths of 9.5, 5.7, and 3.3 mm. A dipole anisotropy corresponding to a motion of 365 km s^{-1} through a 2.735 K blackbody has been subtracted from the maps shown in Fig. 1.

SMOOT et al. (see 371, L4)

© American Astronomical Society • Provided by the NASA Astrophysics Data System

1991ApJ...371L...1S

fluctuations of material that interacts electromagnetically at surface of last scattering is limited to $\Delta\rho_B/\rho_B < 3\Delta T/T_0 < 10^{-4}$ (95% confidence limit) for angular scales $> 7°$ (Silk 1967, 1968).

These anisotropy results provide new limits on the spectrum of long-wavelength energy density fluctuations in the early universe. In particular, the DMR results limit the amplitude of the scale-invariant energy density fluctuations expected in the inflationary cosmology to $\epsilon_H < 3 \times 10^{-5}$ (95% confidence limit) (Abbott & Wise 1984; Górski 1991). This limit generally holds for all fluctuations that are larger than the horizon size at the surface of last scattering.

The DMR instrument is expected to continue operating and improving the experimental results until it is shut off. At the end of 2 yr of operation we can expect sensitivities on the order of $\Delta T/T_0 = 2 \times 10^{-5}$ per 7° field of view, improved calibration, and improved limits on possible systematic effects on the maps and results.

The National Aeronautics and Space Administration/Goddard Space Flight Center (NASA/GSFC) is responsible for the design, development, and operation of the Cosmic Background Explorer. GSFC is also responsible for the software development through to the final processing of the space data. We gratefully acknowledge the many workers whose contributions ensured the success of the *COBE* mission.

REFERENCES

Abbott, L. D., & Wise, M. B. 1984, ApJ, 282, L47
Barrow, J. D., Juszkiewicz, R., & Sonoda, D. H. 1985, MNRAS, 213, 917
Bennett, C. L., et al. 1991, in preparation
Boggess, N. W., et al. 1991, in preparation
Burke, W. L. 1975, ApJ, 196, 329
Cheng, E. S., et al. 1990, Bull. APS, 35, 971
Collins, C. B., & Hawking, S. W. 1973, MNRAS, 162, 307
Fich, M., Blitz, L., & Stark, A. 1989, ApJ, 342, 272
Fixsen, D. J., Cheng, E. S. & Wilkinson, D. T. 1983, Phys. Rev. Letters, 50, 629
Górski, K. 1991, ApJ, 370, L5
Gush, H. P., Halpern, M., & Wishnow, E. 1990, Phys. Rev. Letters, 65, 937
Kerr, F. J., & Lynden-Bell, D. 1986, MNRAS, 221, 1023
Lubin, P., Villela, T. Epstein, G., & Smoot, G. F. 1985, ApJ., 298, L1
Mather, J. C., et al. 1990, ApJ, 354, L37
Partridge, R. B. 1988, Rep. Prog. Phys., 51, 647
Peebles, P. J. E., & Wilkinson, D. T. 1968, Phys. Rev., 174, 2168
Silk, J. 1967, Nature, 215, 1155
———. 1968, ApJ, 151, 459
Smoot, G. F., et al. 1990, ApJ, 360, 685
Stebbins, A. 1988, ApJ, 327, 584
Strukov, I. A., & Skulachev, D. P. 1988, Ap. Space Phys. Rev., 6, 147
Torres, S., et al. 1989, in Data Analysis in Astronomy III, ed. V. Di Gesu et al. (New York: Plenum), p. 319
Toral, M., et al. 1989, IEEE Trans. Ant. Prop., AP-37, 171
Yahil, A., Tamman, G., & Sandage, A. 1977, ApJ, 217, 903
Wilkinson, D. T. 1986, Science, 232, 1517

© American Astronomical Society • Provided by the NASA Astrophysics Data System